Study on Shunt State of Track Circuit Based on Transient Current

QI Huan, ZHANG You-peng, ZHAO Bin
School of Automatic & Electrical Engineering
Lanzhou Jiaotong University
Lanzhou 730070,China
jiay151@163.com

Abstract: - Track circuit is considered to be one of the means of train detection, its shunt state often misjudged due to the shunt malfunction. Aim at the influence of shunt malfunction on the shunt state of track circuit, a detection method for the shunt state of track circuit according to the transient current was proposed. And the time response of track circuit was obtained by the precise time-integration method. The truncation error is efficiently decreased by interlacing the voltage and current nodes along the *x*-axis. Taking the boundary conditions of track circuit in adjusting and shunting state, changes of the receiving end current was simulated. The results show that the precise time-integration is unconditional stability, which is an effective method for analysis of track circuit and the transient current when a train entering or clearing a track section, which can be regard as an important information for the shunt state of track circuit.

Key-Words: track circuit; shunt state; transient current; precise time-integration method; stability

1 Introduction

In railway signaling systems, the shunt state of track circuit is a track section occupied by train, which is detected frequently according to the electrical shunting detection principle [1]. When a train enters a track section, it creates a short-circuit by the shunt resistance that consists of the material resistance of the wheels and the contact resistance between wheel and rail, thus conducting the current from one rail to the other instead of flowing through the relay at the receiving end of the section (Fig.1). This shunts the relay sufficiently to cause it to release and indicate a train's occupancy. However, in some sections, the shunt resistance goes too high due to rails become rusty or dirty, which making the signal amplitude at receiving end is greater than the drop value of the relay, and the signal fails to indicate the presence of the train in the section and gives false information advising approaching trains that the section is clear. This situation is called a shunt malfunction, which is the main cause of a fail to detect a train in a track section and can lead to serious adverse effect on railway transport safety and efficiency. And according to the statistical data released by Chinese railway department, there were about 28 thousand shunt malfunction happening in the Chinese railways [6]. The majority of this fault was caused by excessive shunt resistance[19]. So it's necessary to study on shunt state of track circuit.

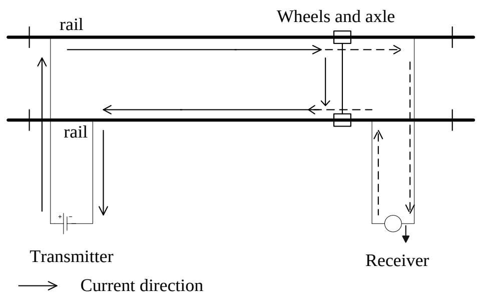

Fig.1 Basic structure of track circuit (occupied)

In order to against this phenomenon, although there has been numerous attempts to prevent shunting malfunction, such as use of the rail surface derusting machine or supersonic arc spraying equipment[2],[3], which requires periodically inspected and shorten rails utility longevity. In some of them[4],[5], train presence is detected by combining with the axle counter train detection technology or poor shunting early warning system, ect. These methods require the additional equipment, high cost; furthermore, the axle counter is vulnerable to the interference of external factors (the track state, weather, and other environmental conditions). Some other solutions use impulse track circuit, which needs to replace the equipment of track circuit, a large amount of construction [6],[7]. Summing up, all these methods, without a total eradication could be obtained, still needs to rely on artificial administration. As shunt malfunction have potential repercussion on signalling and traffic control, therefore, it is necessary to research on the detection method of shunt state of track circuit.

Based on the essence change of track circuit state is the abrupt change of characteristic impedance [8]. In other words, this is the process of the transient signal within track circuit. To realize reliable detection of the track circuit's shunt state, a transient response analysis to the receiving end current signal is proposed in this paper. In order to analyze transient current of track circuit when a train enters a track section. a transient model of track circuit is established based on uniform transmission line theory. Up to now, the common approach for transient analysis of lossy transmission line is using numerical solution method, Such as Fast Fourier Transform (FFT), Numerical Inverse Laplace Transform (NILT) or Finite Difference Time Domain (FDTD), [9-12], ect. However, for coupled lines of track circuit, using FFT or NILT, which may be need a large number of frequency date points to ensure the accuracy of simulation results. And FDTD must ensure the stability of the algorithm. Ref.[13],[14] shows that the precise time-integration method is an efficient and accurate approach for the transient analysis of lossy transmission line, which not only improves the solution accuracy, but also the stability property of the integration algorithm. So, this method for analysis the current response of the shunt state of track circuit is proposed in this paper.

This paper is organized as follows. Section 1 gives an overall background and introduces the problem. Section 2 gives a description of track circuit transient model. Section 3 gives the calculation method for the transient current of track circuit based on the precise time-integration. Section 4 gives the simulation analysis. Finally, Section 5 gives the conclusion.

6 Track Circuit Transmission Line Model

In accordance with the characteristics of track circuit, when you analyze the transient response of the track circuit, the rail line is equivalent to uniform distributed parameter circuit, which composed of three wires includes two rails and the ground. The rail has a longitudinal impedance and mutual inductance, the ground as a conductor which has a large cross-section area and the impedance is zero.

Based on uniform transmission line theory, the rail line model is considered as distributed model that is made of numerous tiny units Δx , the equivalent model of the per-unit as shown in Fig.2. Here R_0 is the rail resistance, Ω/km ; L_0 is the rail inductance, H/km ; M_0 is the mutual inductance between the rails, H/km ; g_0 is the leakage conductance between the rail with the ground,($\Omega\cdot$km)$^{-1}$; g_{12} is the leakage conductance between the rails, ($\Omega\cdot$km)$^{-1}$; C_0 is the leakage capacitance between the rail with the ground, F/km ; C_{12} is the leakage capacitance between the rails, F/km ; x is the distance to the terminal of rail line, km ; $i_1(x,t)$, $i_2(x,t)$ is the current in two rails, respectively, A ; $u_1(x,t)$ 、 $u_2(x,t)$ is the voltage to ground in two rails, respectively, V。

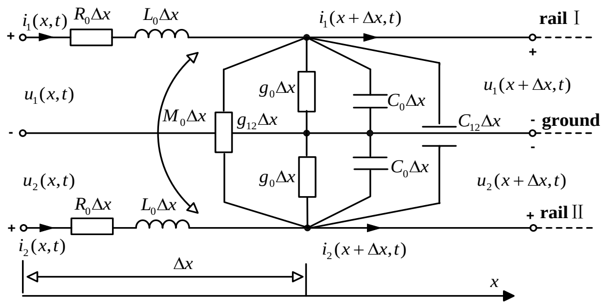

Fig.2 The equivalent model of the rail line

For the model, under the Kirchhoff's voltage and current Laws, the distributions of voltage and current on the rail line can be expressed as Eq.1 when $\Delta x \to 0$.

$$-\frac{\partial u_1(x,t)}{\partial x} = R_0 i_1(x,t) + L_0\frac{\partial i_1(x,t)}{\partial t} + M_0\frac{\partial i_2(x,t)}{\partial t} \tag{1.1}$$

$$-\frac{\partial u_2(x,t)}{\partial x} = R_0 i_2(x,t) + L_0\frac{\partial i_2(x,t)}{\partial t} + M_0\frac{\partial i_1(x,t)}{\partial t} \tag{1.2}$$

$$-\frac{\partial i_1(x,t)}{\partial x} = g_0 u_1(x,t) + g_{12}[u_1(x,t)-u_2(x,t)] + C_0\frac{\partial u_1(x,t)}{\partial t} + C_{12}\frac{\partial [u_1(x,t)-u_2(x,t)]}{\partial t} \tag{1.3}$$

$$-\frac{\partial i_2(x,t)}{\partial x} = g_0 u_2(x,t) + g_{12}[u_2(x,t)-u_1(x,t)] + C_0\frac{\partial u_2(x,t)}{\partial t} + C_{12}\frac{\partial [u_2(x,t)-u_1(x,t)]}{\partial t} \tag{1.4}$$

The above partial differential equations can be described in matrix form as:

$$-\frac{\partial \boldsymbol{u}(x,t)}{\partial x} = \boldsymbol{R}\boldsymbol{i}(x,t) + \boldsymbol{L}\frac{\partial \boldsymbol{i}(x,t)}{\partial t} \tag{2.1}$$

$$-\frac{\partial \boldsymbol{i}(x,t)}{\partial x} = \boldsymbol{G}\mathbf{u}(x,t) + \boldsymbol{C}\frac{\partial \boldsymbol{u}(x,t)}{\partial t} \quad (0 \le x \le l) \tag{2.2}$$

where l is the length of the rail line; $\boldsymbol{u}(x,t)$ =[$u_1(x,t)$ $u_2(x,t)$]$^{\mathrm{T}}$; $\boldsymbol{i}(x,t)$ =[$i_1(x,t)$ $i_2(x,t)$]$^{\mathrm{T}}$; $\boldsymbol{u}(x,t)$, $\boldsymbol{i}(x,t)$ is the voltage and current matrix along the rail line, respectively; $\boldsymbol{R}$、$\boldsymbol{L}$ are the per-unit length matrix of resistance and inductance; $\boldsymbol{G}$、$\boldsymbol{C}$ are the per-unit length matrix of conductance and capacitance.

$$\boldsymbol{R}=\begin{bmatrix} R_0 & 0 \\ 0 & R_0 \end{bmatrix};\quad \boldsymbol{G}=\begin{bmatrix} g_0+g_{12} & -g_{12} \\ -g_{12} & g_0+g_{12} \end{bmatrix};$$

$$\boldsymbol{L}=\begin{bmatrix} L_0 & M_0 \\ M_0 & L_0 \end{bmatrix};\quad \boldsymbol{C}=\begin{bmatrix} C_0+C_{12} & -C_{12} \\ -C_{12} & C_0+C_{12} \end{bmatrix};$$

It is clear that the change of voltage and current along the rail line at any time can be described by the solutions of the above transmission line equations. Therefore, to solve the transmission line equations is the basis for the transient analysis of track circuit.

6 Time Response of Track Circuit

Track circuit is a lossy transmission line. The precise time-integration method enables one to overcome the difficulty of taking into account the open or short boundaries by traditional methods. In addition, the benefit of the time domain model accounts for arbitrary initial conditions[15],[16]. So this provides an efficient numerical approach to solve the transient response of track circuit.

3.1 Space Discretization of Transmission Line Equations

In this section one crucially needs to solve the transmission line equations of track circuit, as shown in Eq.(2). First, by implementing the discretization in the space coordinate(x) to Eq.(2). The classical discrete method where the samples of both voltages and currents are taken at the same points[13]. In addition, voltages and currents partial derivative respectively used forward difference and backward difference, which causes truncation error is:

$$R[y]=\pm\frac{l^2}{2M}y''(\xi_i) \tag{3}$$

To reduce the truncation error, the voltage and current is sampled by interlacing the voltage and current nodes along x-axis in this paper (as shown in Fig.3).

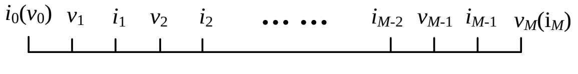

Fig 3 Interval sampling of voltage and current

We divide the transmission line into $2M$-1 sections each of length Δx =$l/(2M$-1), at the beginning and end points, the partial derivative of the voltage and current to x is approximated by the forward differential and backward difference respectively. While at each discrete point k ($k=1,2,...M-1$), the centered difference scheme is used. So we can obtain the following questions:

$$\frac{\mathrm{d}\boldsymbol{u}_k(t)}{\mathrm{d}t}=-\boldsymbol{C}^{-1}\frac{\boldsymbol{i}_k(t)-\boldsymbol{i}_{k-1}(t)}{2\Delta x}-\boldsymbol{C}^{-1}\boldsymbol{G}\boldsymbol{u}_k(t) \tag{4.1}$$

$$\frac{\mathrm{d}\boldsymbol{i}_k(t)}{\mathrm{d}t}=-\boldsymbol{L}^{-1}\frac{\boldsymbol{u}_{k+1}(t)-\boldsymbol{u}_k(t)}{2\Delta x}-\boldsymbol{L}^{-1}\boldsymbol{R}\boldsymbol{i}_k(t) \tag{4.2}$$

where: k=1,2$\cdots M$-1, $\boldsymbol{u}_k(t)=\boldsymbol{u}(k\Delta x,t)$; $\boldsymbol{i}_k(t)=\boldsymbol{i}(k\Delta x,t)$.

$$\frac{\mathrm{d}\boldsymbol{u}_M(t)}{\mathrm{d}t}=-\boldsymbol{C}^{-1}\frac{\boldsymbol{i}_M(t)-\boldsymbol{i}_{M-1}(t)}{\Delta x}-\boldsymbol{C}^{-1}\boldsymbol{G}\boldsymbol{u}_M(t) \tag{4.3}$$

$$\frac{\mathrm{d}\boldsymbol{i}_0(t)}{\mathrm{d}t}=-\boldsymbol{L}^{-1}\frac{\boldsymbol{u}_1(t)-\boldsymbol{u}_0(t)}{\Delta x}-\boldsymbol{L}^{-1}\boldsymbol{R}\boldsymbol{i}_0(t) \tag{4.4}$$

For the same length of transmission line, this method effectively reduced the space step length to be compared with method in Ref.[7], and the centered difference causes truncation error is:

$$R[y]=\frac{l^2}{6\times(2M-1)^2}y'''(\xi_i) \tag{5}$$

which is significantly smaller than Eq.3.

3.2 Time Precise Integration for Solving the Transmission Line Equations

For Eq.(4) we can describe in matrix form as :

$$\frac{\mathrm{d}\boldsymbol{X}}{\mathrm{d}t}=\boldsymbol{H}\boldsymbol{X}+\boldsymbol{F} \tag{6}$$

where: $\boldsymbol{X}=[\boldsymbol{u}_1,\boldsymbol{u}_2,\boldsymbol{u}_3...\boldsymbol{u}_M,\boldsymbol{i}_0,\boldsymbol{i}_1...\boldsymbol{i}_{M-1}]^{\mathrm{T}}$;

$\boldsymbol{F}=[0,...0,-\boldsymbol{C}^{-1}\boldsymbol{i}_M/\Delta x,\boldsymbol{L}^{-1}\boldsymbol{u}_0/\Delta x,0,...,0]^{\mathrm{T}}$; $\boldsymbol{H}$ as shown in next page.

We can obtain the solution of Eq.(6) as:

$$\boldsymbol{X}(t)=\exp(\boldsymbol{H}\cdot t)\boldsymbol{X}(0)+\int_0^t\exp[\boldsymbol{H}\cdot(t-\tau)\boldsymbol{F}(\tau)]\mathrm{d}\tau \tag{7}$$

where $\boldsymbol{X}(0)$ represent the state initial value. In order to satisfy the demands of the precise integration, the time be divided into a series of small time step: $t_j=jh$, $j=0,1,2...$, when $t=t_j$, there is:

$$\boldsymbol{X}(t_j)=\boldsymbol{X}^j=\exp(\boldsymbol{H}\cdot jh)\boldsymbol{X}(0)+\int_0^{jh}\exp[\boldsymbol{H}\cdot(jh-\tau)\boldsymbol{F}(\tau)]\mathrm{d}\tau \tag{8}$$

Suppose h is sufficiently small, inhomogeneous $\boldsymbol{F}$ can be approximated as a constant within the time-interval (t_j,t_{j+1}), so we have:

$$\begin{aligned}\boldsymbol{X}(t_{j+1})=\boldsymbol{X}^{j+1}&=\exp(\boldsymbol{H}\cdot(h))[\boldsymbol{X}^j+\boldsymbol{H}^{-1}\boldsymbol{F}^j]-\boldsymbol{H}^{-1}\boldsymbol{F}^j\\&=\boldsymbol{T}\cdot[\boldsymbol{X}^j+\boldsymbol{H}^{-1}\boldsymbol{F}^j]-\boldsymbol{H}^{-1}\boldsymbol{F}^j,\ j=0,1,2...\end{aligned} \tag{9}$$

$$
\boldsymbol{H}=\left[\begin{array}{ccccccc|cccccc}
-\boldsymbol{C}^{-1}\boldsymbol{G} & & & & & & & \frac{\boldsymbol{C}^{-1}}{2\Delta x} & -\frac{\boldsymbol{C}^{-1}}{2\Delta x} & & & & \\
 & \cdot & & & & & & & \cdot & \cdot & & & \\
 & & \cdot & & & & & & & \cdot & \cdot & & \\
 & & & \cdot & & & & & & & \cdot & \cdot & \\
 & & & & \cdot & & & & & & & & \\
 & & & & & \cdot & & & & & \frac{\boldsymbol{C}^{-1}}{2\Delta x} & & -\frac{\boldsymbol{C}^{-1}}{2\Delta x} \\
 & & & & & & -\boldsymbol{C}^{-1}\boldsymbol{G} & & & & & & \frac{\boldsymbol{C}^{-1}}{\Delta x} \\
\hline
-\frac{\boldsymbol{L}^{-1}}{\Delta x} & & & & & & & -\boldsymbol{L}^{-1}\boldsymbol{R} & & & & & \\
\frac{\boldsymbol{L}^{-1}}{2\Delta x} & -\frac{\boldsymbol{L}^{-1}}{2\Delta x} & & & & & & & \cdot & & & & \\
 & \cdot & \cdot & & & & & & & \cdot & & & \\
 & & \cdot & \cdot & & & & & & & \cdot & & \\
 & & & \cdot & \cdot & & & & & & & \cdot & \\
 & & & & \frac{\boldsymbol{L}^{-1}}{2\Delta x} & & -\frac{\boldsymbol{L}^{-1}}{2\Delta x} & & & & & & -\boldsymbol{L}^{-1}\boldsymbol{R}
\end{array}\right]
$$

For the matrix $\boldsymbol{T}$ can be computed by the precise integration. Based on the identity

$$\boldsymbol{T}=\exp(\boldsymbol{H}\cdot(h))=\exp[\boldsymbol{H}\cdot(h/m)]^m$$

where: $m=2^N$, $\Delta t=h/m$, h is sufficiently small. Within the time $\Delta t=h/2^N$, taking the four-order Taylor expansion, the $\exp(\boldsymbol{H}\cdot\Delta t)$ can be approximated as:

$$\exp(\boldsymbol{H}\cdot\Delta t)\approx\boldsymbol{I}+\boldsymbol{H}\Delta t+(\boldsymbol{H}\Delta t)^2/2+(\boldsymbol{H}\Delta t)^3/3!+(\boldsymbol{H}\Delta t)^4/4!$$
$$=\boldsymbol{I}+\boldsymbol{Ta} \qquad (10)$$

For $\boldsymbol{T}=\exp(\boldsymbol{H}\cdot(h))=(\boldsymbol{I}+\boldsymbol{Ta})^{2^N}$, which can be analysis into $\boldsymbol{T}=(\boldsymbol{I}+\boldsymbol{Ta})^{2^{N-1}}\times(\boldsymbol{I}+\boldsymbol{Ta})^{2^{N-1}}$, the total decomposition of N times, which is equivalent to perform the following statement:

$$\text{for}(i=0;i<N;i++)\ \boldsymbol{Ta}=2\boldsymbol{Ta}+\boldsymbol{Ta}\times\boldsymbol{Ta};$$

Then, we can get $\boldsymbol{T}=\boldsymbol{I}+\boldsymbol{Ta}$. Since Δt is very small, Eq.(10) within the accuracy range of the computer, which can be regard as the exact solution of exponential function $\boldsymbol{T}$.

3.3 Stability Analysis of the Precise Time Integration Method

Considering the solution of the homogeneous equation of Eq.6, we have a recursive scheme as

$$\boldsymbol{X}^{n+1}=e^{\boldsymbol{H}\Delta t}\boldsymbol{X}^{n} \qquad (11)$$

The stability of the precise integration method can be determined with so-called Fourier method, which is identified with the follow inequality:

$$\left|e^{\lambda_i\Delta t}\right|\le 1 \qquad (12)$$

where λ_i is all the eigenvalues of $\boldsymbol{H}$. Apparently, as long as $\mathrm{Re}(\lambda_i\Delta t)\le 0$, the inequality (12) can be satisfied. Since the time-step Δt is a positive real, for the inequality can be satisfied only if $\mathrm{Re}(\lambda_i)\le 0$. That is to say, the time-step size Δt does not exert an influence on the stability of the scheme, and the Eq.12 is determined only with the sign of $\mathrm{Re}(\lambda_i)$. So, the time precise integration method is unconditionally stable regardless of the time-step size.

6 Simulation Analysis

Due to the shunt state of track circuit is based on the adjusting state, for further analysis of the transient current when train enters the track section, the first thing is calculated the adjusting state.

4.1 Analysis of the Adjusting State

The simple equivalent circuit of track circuit as shown in Fig.4, where in the beginning with the voltage source U_{s} and Z_{s} act as internal resistance; the terminal is connected with the load impedance Z_{L}, $i(t)$ is the received current; R_{f} is the equivalent shunt resistance.

The different working states of track circuit correspond to different boundary conditions. When the track section is unoccupied, track circuit in the adjusting state.

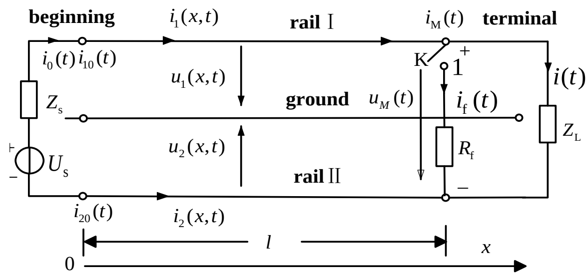

Fig.4 The equivalent circuit of track circuit

At this point, K disconnects the contact 1, the beginning and terminal boundary conditions of track circuit are as follows:

beginning: $u_0(t) = F_1[i_0(t), U_S(t)] = U_s(t) - i_0(t) Z_s$,

where: $i_0(t) = i_{10}(t) = -i_{20}(t)$;

terminal: $i(t) = i_M(t) = F_2[u_M(t)]$

$$= u_M(t) / Z_L = (u_{1M}(t) - u_{2M}(t)) / Z_L;$$

Consider the initial condition $\boldsymbol{X}(0)$ =0, the space and time step size is respectively: M=100; h =1e-3s. N=20. and the main parameters of track circuit are shown in Table 1.

Table 1: the main parameters of track circuit

Parameter name	Parameter value
Rail type	P60
Supply voltage	30 V
Internal resistance	0.1Ω
Length	1.2 Km
The load	2.7Ω

Fig.5 shows the current response at the receiving end of track circuit. To demonstrate the validity of the precise time-integration compared its simulation result with the finite difference time domain (FDTD).

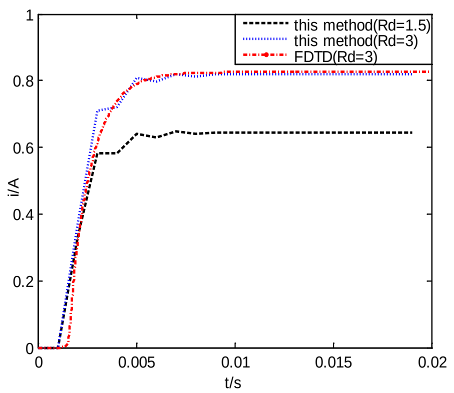

Fig.5 Current response of the receiving end

It can be seen that the current signal quickly comes to stability with time passes, and the current value becomes larger with increased ballast resistance under other parameters maintained a fixed value. This is due to when ballast resistance increases; the leakage current is reduced during the process of signal transmission. It is also seen that the precise time-integration method is agreement with the direct solutions by the FDTD method.

4.2 Analysis of the Shunt State

From the above analysis, substituting the boundary and initial conditions of adjusting state into Eq.(9). We can get the steady state value of the voltage and current along the rail line, which can be used as the initial condition of the shunt state of track circuit, and further analysis the current response by combing with the boundary condition of shunt state.

When a train penetrates the track section, its wheels and axles act as a shunt resistance R_f, in Fig.4, K connects with contact 1. This time, the beginning boundary condition of track circuit is the same as the adjusting state:

$$u_0(t) = F_1[i_0(t), U_S(t)] = U_s(t) - i_0(t) Z_s,$$

where: $i_0(t) = i_{10}(t) = -i_{20}(t)$;

While in the terminal of track circuit, current flow to the receiver changed as:

$$i(t) = i_M(t) \times R_f / (R_f + Z_L)$$
$$= F_2[u_M(t)] \times R_f / (R_f + Z_L)$$

As is often the case, the shunt resistance R_f is very small (0.04-0.15Ω)[17], $R_f << Z_L$, so compared with the adjusting state, the receiving end of current decreases obviously.

When the train is arriving at the beginning and will leave the section, the equivalent circuit of track circuit as shown in Fig.6. At this moment, the boundary conditions of track circuit in the beginning and terminal, respectively:

$$u_0(t) = F_1[i_0(t), U_S(t)] = U_s(t) - i_0(t) Z_s,$$

where: $i_0(t) = i_{10}(t) + i_f(t) = i_{10}(t) + u_0(t) / R_f$;

$$i(t) = i_M(t) = F_2[u_M(t)] = u_M / Z_L$$
$$= u_M / Z_L = (u_{1M}(t) - u_{2M}(t)) / Z_L$$

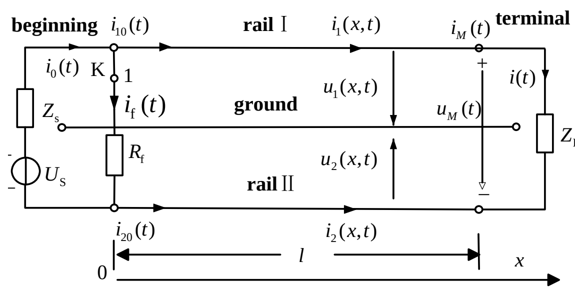

Fig.6 The equivalent circuit of track circuit

When the train leaving, in Fig.6, open the contact 1 and track circuit to the adjusting state.

.2.1 Normal Shunt Section

Based on the above conditions, Fig.7 indicates the current response of the receiver when a train is shunting on the rails at *t*=20ms, where R_f =0.06 Ω , R_d=1.5 Ω·km . It can be seen that, at *t*=20ms, because of shunting effect of R_f , the amplitude of current decreases dramatically, (there will be a fall edge), which is a transient process of current signal.

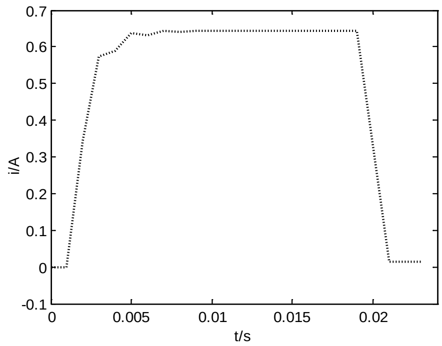

Fig.7 Current response of a train entering the track section

Fig.8 shows when a train passing through the track section, current response of the receiver.

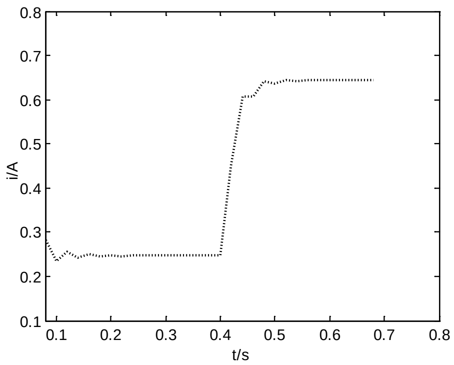

Fig.8 Current response of a train leaving the track section

It's also can be seen that, at *t*=40ms, the current signal at the receiving end of track circuit increases sharply, (there will be a rising edge), which is a transient signal.

From Fig.7 and Fig.8, it can be seen that, in the moment of a train entering or leaving the track section, there is a transient signal. As a result, this can be used to detection the shunt state of track circuit by identifying signal type of transient current (fall edge or rising edge).

.2.2 Shunt Malfunction Section

In the practical application, due to the complex working environment, the detection of track circuit's shunt state is easily effected by ballast resistance, supply voltage and shunt resistance [18]. The traditional method may be difficult to be used for train detection. For example, Table 2 shows the received current amplitude under different conditions.

Table 2 the current at receiving end with $f = 1000\text{Hz}$, $l = 1.2\text{km}$, $R_f = 0.1\Omega$

R_d /(Ω·km)	U_S /(V)	R_f(Ω)	Adjusting state *i*/(A)	shunt state *i*/(A)
1.5	30	0.06	0.6439	0.0230
1.5	50	0.06	1.0732	0.0383
100	30	0.06	2.7612	0.0986
100	50	0.06	4.6020	0.1644
1.5	30	2	0.6439	0.2740
100	50	2	4.6020	1.9583

It can be seen from Table 2 that the current amplitude increases with the increase of supply voltage, ballast resistance and shunt resistance. Especially in the shunt malfunction section, mainly due to the rust or dirt of rail (or wheel) surface that make the shunt resistance beyond the standard values[19]. In such a situation, if we comparing the variation of received current amplitude with a certain threshold, which may be difficult [20].

Fig.9 shows the change of current from the adjusting state to the shunt state occurs at the worst conditions of shunt model (in this case, consider the rail type is P60, the supply voltage is 50V, and with the largest ballast resistance R_d =100 Ω·km and R_f=2 Ω).

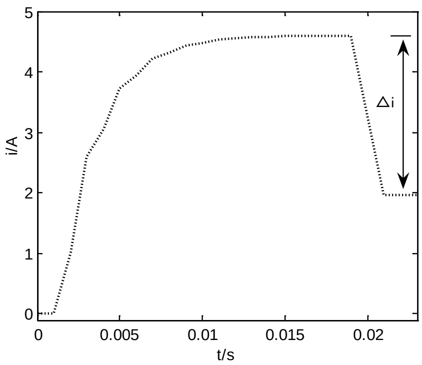

Fig.9 Current response in the bad condition

It can be seen that, in shunt malfunction section, the variation of current amplitude (Δi) is smaller than the variation of current amplitude in Fig 6. That may be cause a false judgment if the train detection by the traditional method. However, despite the variation of current amplitude (Δi) decreases, there still is a transient change process, at *t*=18ms. Therefore, the transient characteristics of current signal, which can be used for train detection, even in the shunt malfunction section.

5 Conclusion

Aiming at the shunt malfunction problem, a transient response analysis for the shunt state of track circuit based on the precise time-integration method is proposed in this paper. Combined with the different initial and boundary conditions of track circuit, by numerical simulating analysis the current response from the adjusting state to the shunt state. The theoretical and simulation results show that the precise time-integration algorithm is an effective method for the analysis of shunt state of track circuit, and when a train enters a track section, there is obviously transient current even in the worst conditions of shunt state. So this is important information for the shunt state of track circuit.

6 ACKNOWLEDGEMENTS

This project is supported by the China Railway Corporation and Technology Research and Development Program (2015X0007-H).

References:

[1] F.Houze, Electrical behaviour of the wheel-rail contactin, Electrical Contacts & International Conference on, 2012, 67-72.

[2] LUO Yong, Simple Analysis and Solution of Bad Track Circuit Shunting, Railway Signaling & Commubication engineering, 2004, 21(6):23.

[3] HE Gui-yang, HUA Ze-xi, Solution analysis for defective shunting of track circuit, Railway Computer Application, 2012, 21(1):48-50.

[4] LI Ming, Investigation the axle counter to solve the bad shunting of track circuit, Railway Signaling & Commubication engineering, 2013, 10(6):58-60.

[5] MI Gen-suo, WANG Yan-kuai, WANG Wen-bo, Application of Radar Chart in Poor Shunting Early Warning for Track Circuit, Journal of the China Railway Society, 2013, 35(11): 66-70.

[6] YUAN Xiao-jun, Research on Shunt Malfunct-ion of Railway Track Circuit, Railway Signal and Communication, 2007, 43(4): 11-14

[7] DI Jing-jing, Study on the New Asymmetric Pulse Track Circuit Technology, Xi'an University of Architecture &Technology, 2012.

[8] ZHAO Bin, ZHANG You-peng, WEI Lei, Analysis on the Time Responses of Track Circuits, Journal of the China Railway Society, 2014, 36(9):68-71.

[9] C.R.Paul, Analysis of Multiconductor Transmi-ssionon Lines, New York: Wiley Interscience, 1994.

[10] A.Orlandi, C.R.Paul, FDTD Analysis of Lossy Multiconductor Transmission Lines Terminated in Arbitrary Loads, IEEE Trans, On Electromagnetic Combatibility, vol. 38, no. 3, Aug. 1996, pp.388-399.

[11] P.Gómez and F.A.Uribe, “The numerical Laplace transform: An accurate tool for analyzing electromagnetic transients on power system devices,” Int.J.Elect.Power Energy Syst.,vol.31,no.2–3,pp.116–123,Feb./Mar.2009.

[12] P. Moreno and A. Ramírez, “Implementation of the numerical Laplace transform: A review,” IEEE Trans. Power Del., vol. 23, no. 4, pp.2599–2609, Oct. 2008.

[13] ZHAO Jin-quan, MA Xi-kui, QIU Guan-yuan, A Precise Time-Integration for Analysis of Time-Domain Response to Lossy Transmission Lines, Microelectronics, 1997, 27(3):181-185.

[14] KONG Xiang-dong, ZHONG Wan-xie, Precise time integration algorithm of stiff equation in nonlinear dynamic system, Journal of Dalian University of Technology, 2002, 42(6):654-658.

[15] ZHAO Jin-quan, MA Xi-kui, QIU Guan-yuan. A Precise Computation Method for the Time-Domain Response of Multiconductor Coupled Transmission Lines, Journal of Circuit and Systems, 1997, 2(3):13-17.

[16] TANG Min, MA Xi-kui, A Precise Integration Algorithm for Transient Simulation of Interco-nnects in High-Speed VLSI, Journal of Electro-nica, 2004, 32(5): 787-790.

[17] Z. Yong-xian, X. Xue-song, and Y. Jiang-song, “Modeling and simulation of ZPW-2000A jointless track circuit,” Journal of East China Jiaotong University, no.3, pp.64–68, 2009.

[18] C. J. Baker, L. Chapman, A. Quinn, and K. Dobney, “Climate change and the railway industry: a review,” Proceedings of the Institution of Mechanical Engineers C: Journal of Mechanical Engineering Science, vol.224, no.3, pp.519–528, 2010.

[19] SUN Shang-peng, ZHAO Hui-bing, CHEN De-wang, ect, Research on Method for Calculation of Shunt Resistances of Track Circuit Using Electrical Contact Theory, Journal of the China Railway Society, 2014, 36(3): 32-35.

[20] F. Filippone, A. Mariscotti, and P. Pozzobon, “The internal impedance of traction rails for DC railways in the 1–100 kHz frequency range,” IEEE Trans. Instrum. Meas., vol. 55, no. 5, pp. 1616–1619, Oct. 2006.